Biochimica et Biophysica Acta 813 (1985) 213–220
Elsevier

BBA 72479

Significant potassium ion accumulation at the external surface of *Myxicola* giant axons

Nava Moran [a,*], Emanuel Levitan [a], Yoram Palti [a], Priscilla Roslansky [b] and William J. Adelman, Jr. [b]

[a] *Department of Physiology and Biophysics, The Rappaport Family Institute for Research in Medical Sciences, Technion, Haifa (Israel) and* [b] *Laboratory of Biophysics, NINCDS, NIH, at the Marine Biological Laboratory, Woods Hole, MA (U.S.A.)*

(Received November 5th, 1984)

Key words: Ion accumulation; Voltage clamp; K^+ transport; Nerve membrane; (*Myxicola* giant axon)

Potassium accumulation associated with outward membrane potassium current was investigated experimentally in *Myxicola* giant axon. During prolonged voltage-clamp pulses to positive transmembrane potentials, the K^+ equilibrium potential may approach zero mV, suggesting massive K^+ accumulation outside the axonal membrane to concentrations many-fold higher than those in the bathing medium. The potassium accumulation can be satisfactorily described by a three-compartment model, consisting of the nerve fiber, a restricted physiological periaxonal space and the bulk solution. The average thickness, θ, of the periaxonal space is calculated as 177 ± 59 Å, i.e., comparable to that in the squid, while the permeability coefficient of the external barrier, P_{K_s}, was calculated to be $(1.4 \pm 0.4) \cdot 10^{-4}$ cm/s. These conclusions are well supported by morphological study.

Introduction

Ion accumulation at the membrane surface of a voltage-clamped nerve fiber results from differences in the ion transport number values along the current flow pathway [1].

Realizing that the analysis of ion conductance kinetics may be seriously hindered by ion accumulation, Frankenhaeuser and Hodgkin [2] were the first to study potassium ion accumulation in squid axon and to describe it quantitatively in terms of a three-compartment model consisting of (i) the nerve fiber bounded by the axolemma, (ii) the adjacent medium (space) restricted by an external barrier and (iii) the bulk solution. Ion accumulation was subsequently described in detail in the squid giant axon [3,4] and in frog node [5,6].

K^+ accumulation has been dealt with only briefly in *Myxicola* giant axon [7]. The rate of accumulation was reported to be significantly slower than in squid. This was reflected in an apparent periaxonal space thickness of about 2000 Å (Ref. 7, see also Ref. 8), in contrast to the 200–400 Å space found in a squid [3,4,9].

In this study, we show that the rate of potassium accumulation at the surface of *Myxicola* axons may be comparable to that in squid.

Preliminary results have appeared in an abstract form [10].

Materials and Methods

Giant axons from *Myxicola infundibulum* (from Marine Res. Assoc. N.B., Canada) were dissected,

* To whom correspondence should be addressed at: Laboratory of Biophysics, National Institutes of Health, Bldg. 36, Rm. 2A29, Bethesda, MD 20205, U.S.A.

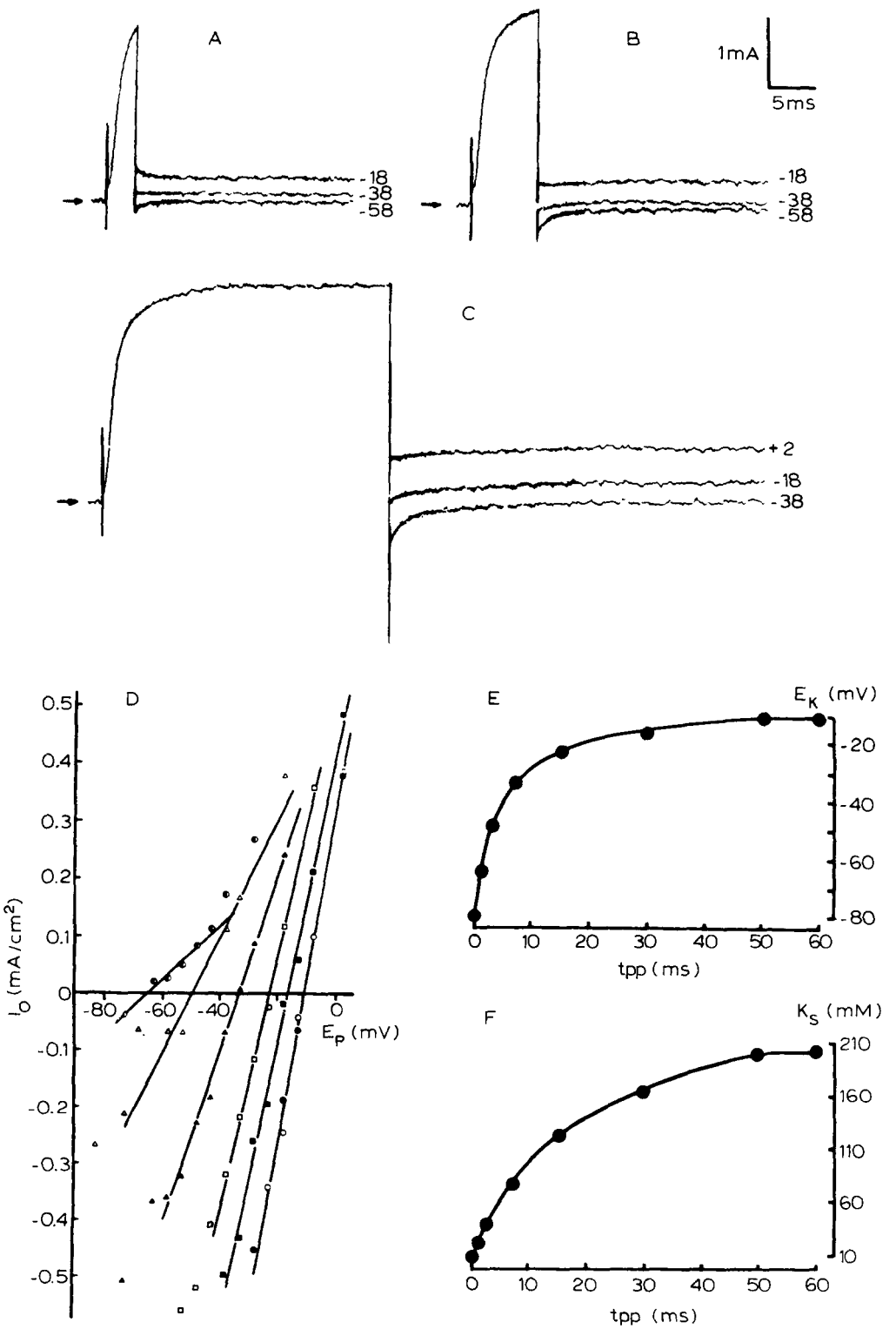
A
B
1mA
5ms
-18
-38
-58
-18
-38
-58
C
+2
-18
-38
D
0.5
0.4
0.3
0.2
0.1
0
-0.1
-0.2
-0.3
-0.4
-0.5
-80
-60
-40
0
E_P (mV)
I_o (mA/cm²)
E
E_K (mV)
-20
-40
-60
-80
0
10
20
30
40
50
60
tpp (ms)
F
K_S (mM)
210
160
110
60
10
0
10
20
30
40
50
60
tpp (ms)

stretched (1.5 ×) and mounted as described in Ref. 11. The lucite and voltage-clamp set-up were similar to those described in Ref. 12. The artificial sea-water consisted of 430 mM NaCl/10 mM KCl/10 mM $CaCl_2$/50 mM $MgCl_2$/5 mM Tris-HCl (pH 7.4)/$6 \cdot 10^{-7}$ M tetrodotoxin (Sigma, U.S.A.). Temperature ranged between 2 and 7°C (constant to within 0.5°C in a single experiment).

The voltage-clamp experiments were carried out under digital computer control (Data General, Nova 800). The holding potential (equaling the resting potential) was adjusted manually. Membrane currents were sampled at a rate (adapted to the rate of change of the current) of between 30 and 5 kHz.

All currents were corrected for leakage, using a value of leakage conductance (g_L) determined with a hyperpolarizing pulse of −70 mV, based on the assumption that g_L is constant in the range of potential used [13]. In the following experiments, g_L was between 1 and 2 mS.

Partial smoothing of noise was achieved using the running average method (3-points bin).

Myxicola giant axons, dissected as described above, were fixed in 1% OsO_4 by the method of Villegas [16] as modified by Adelman et al. [15], and stained with 2% uranyl acetate, en block. Following dehydration and embedding in Epon/Araldite, cross and longitudinal sections were cut and examined in a JEM model 7 electron microscope. Measurements of periaxonal and mesaxonal spaces were made from electron micrographs obtained from these sections. Details of procedures are given by Adelman et al. [15].

Results and Discussion

Potassium accumulation in the periaxonal space

The procedure for measuring the rate and the extent of potassium accumulation in the periaxonal space during membrane depolarization involves determination of reversal potentials for potassium, E_K [2], by the 'tail-current' method [14] depicted in Fig. 1A–E. Fig. 1F illustrates the calculated potassium concentrations in the periaxonal space, K_s, as a function of the duration of conditioning depolarization. As depolarization lengthens, E_K becomes more positive, indicating a growing potassium concentration outside the membrane (from 10 to 202 mM). These results are subsequently analysed in terms of the three-compartment model.

Computation of parameters of accumulation

Within the framework of the threee-compartment model, two parameters define the ion accumulation in the space, namely: θ, the space thickness; and P_{Ks}, the apparent permeability of the external barrier, as shown in the following equation [4]:

$$d\delta K_S/dt = \frac{I_K}{F}(1 - t_{Ks}) - P_{Ks}\delta K_S/\theta \qquad (1)$$

where δK_s denotes the excess of potassium ion in the space over its concentration in the external bulk solution as a function of time, t; t_{Ks}, the transport number of K^+ in the solution within the space, given by: $t_{Ks} = K_S/\Sigma([\text{anions}]_s + [\text{cations}]_s)$; and F the Faraday constant. The parameters θ and P_{Ks} are fitted simultaneously to the time-courses of potassium current, I_K, and of the corresponding concentration changes in the space, δK_S, using the integrated form of the material balance equation (Eqn. 1), as described in detail by Moran et al. [6]. The parameters are fitted for a duration of a step depolarization ranging usually between 1.5 and 15 ms, within the

Fig. 1. The 'tail-current' method for determining potassium reversal potential, E_K [2,11] and the resulting K^+ accumulation in space (K_s). (A–C) Potassium currents during pairs of depolarizing pulses. The prepulse potential, E_{pp}, is +66 mV. The prepulse durations, t_{pp}, are: 3, 7 and 30 ms, in A, B and C, respectively (three pairs of pulses were superimposed in each part). Numbers denote values of the test potentials, E_p values. Note that the tail-currents may reverse their initial sign when t_{pp} lengthens or when E_p changes after the same t_{pp}. Arrows indicate zero holding current. (D) Instantaneous *I-V* relationships for different depolarizing prepulse durations, t_{pp}. The points correspond to zero-time tail-currents, I_0, elicited when membrane potential was stepped from E_{pp} of +18 mV to various test pulses, E_p's. The t_{pp} values are: ◐, 1.5; △, 3; ▲, 7; □, 15; ■, 30; ○, 50 and ●, 60 ms. (E) K^+ equilibrium potential, E_K, as a function of t_{pp}; symbols denote zero-cross-over points of the instantaneous *I-V* relationships. (F) K^+ concentration outside the axonal membrane, K_s, calculated from E_K values (using Nernst relationship and assuming that the internal $[K^+]$ remains constant at 320 mM [20]), as a function of t_{pp}. Lines were fitted by eye.

transient of accumulation. Alternatively, P_{Ks} is determined directly from the steady-state values of I_K and K_S:

$$P_{Ks} = \frac{I_K(1 - t_{Ks})}{F\delta K_S} \quad (2)$$

Consequently, the P_{Ks} parameter is labeled $P_{Ks(t)}$ or $P_{Ks(s)}$, respectively.

The apparent space thickness

Table I summarizes the values of θ evaluated from transients in potassium accumulation. These values were determined simultaneously with the $P_{Ks(t)}$ values.

The magnitude of membrane depolarization, in the range of +70 to +150 mV, does not seem to affect θ in any consistent way. The average θ is 177 ± 59 Å. For comparison, the values for *Loligo pealei* and *Loligo vulgaris* are 360 ± 130 Å [17,5] and 100 Å [9], respectively.

The apparent permeability of the external barrier

In addition, Table I lists the values of P_{Ks} computed by two methods using several depolarizations. It seems that the magnitude of the depolarization does not consistently affect the P_{Ks} values.

The average P_{Ks} value obtained from the steady state, $P_{Ks(s)}$, is: $(1.3 \pm 0.4) \cdot 10^{-4}$ cm/s (as compared with $(3.2 \pm 1.2) \cdot 10^{-4}$ cm/s [17,5] and $2.3 \cdot 10^{-4}$ cm/s [9] in squid), while that derived from potassium accumulation time course, $P_{Ks(t)}$, is $(1.4 \pm 0.4) \cdot 10^{-4}$ cm/s. The difference between the two averages does not appear to be significant. However, when the differences are computed for each axon separately, the average difference is $(0.14 \pm 0.09) \cdot 10^{-4}$ cm/s. A correlated pairs test reveals that the P_{Ks} values determined during steady state are significantly lower than those obtained by the alternative method (with a significance level of between 5 and 10%). This finding may imply that the apparent P_{Ks} or θ values

TABLE I

APPARENT PERMEABILITY, P_{Ks}, AND SPACE THICKNESS, θ, IN *MYXICOLA* GIANT AXONS

The P_{Ks} values were evaluated by two independent methods; $P_{Ks(s)}$ values from the steady-state currents (elicited during various depolarizations, E_{pp}) and from the E_K values; $P_{Ks(t)}$ values from the time courses of their changes (see Materials and Methods). The mean was calculated using a single θ or P_{Ks} value for each axon, or an average value when more than one measurement were performed on a single axon.

Axon number	E_{pp} (mV)	θ (Å	$P_{Ks(t)} \times 10^4$ (cm/s)	$P_{Ks(s)} \times 10^4$ (cm/s)
01	+38	48	0.50	0.28
	+73	60	0.33	0.21
	+103	52	0.11	0.17
02	+31	104	0.95	0.75
	+66	175	0.24	0.64
03	+32	65	0.32	0.28
	+67	40	0.36	0.18
04	+71	110	0.72	0.54
07	+18	661	3.01	3.30
08	+12	163	2.34	1.70
	+42	215	2.14	1.70
	+92	184	2.31	1.90
09	+7	67	1.63	1.10
	+37	114	1.80	1.10
	+87	143	1.59	1.10
10	+86	123	3.0	2.9
11	+11	202	1.24	0.90
	+41	142	0.30	0.34
	+91	129	0.33	0.25
Mean ± S.E.	177 ± 59	1.39 ± 0.37	1.25 ± 0.36	

change during the course of a depolarization. This might be due to the transient effects of electro-osmotic flow [18]. Alternatively, the difference between the values of $P_{Ks(s)}$ and $P_{Ks(t)}$ may be attributed to the (neglected) effect of the unstirred layer external to the sheath surrounding the axon [19].

E_K reconstruction within the framework of the three-compartment model

To check the predictive power of the three-compartment (two parameter) model, Eqn. 1 was used to reconstruct the E_K changes from outward potassium currents measured during various depolarizations. This is illustrated in Fig. 2. The computed E_K values appear to agree reasonably well with the experimental data.

Different estimates of the space thickness by others

Our results seem to be in variance with the values of the space thickness reported by Binstock and Goldman: 2240 ± 730 Å [7] and by Begenisich: 700–4000 Å [8]. The origin of the discrepancy between our findings and those of Binstock and Goldman [7] seems to exist already in the measured values of the E_K shifts, ΔE_K, the latter being clearly smaller than ours. These differences cannot be attributed to the fact that we did not correct for series resistance, R_s, in our experiments, since both the potassium currents used to determine E_K (which were generated by test pulses close to E_K) and leakage currents were very small. For such currents, the maximum error in the actual membrane potential during a test pulse is negligible. For example, the error is 1 mV for a 0.1 mA/cm^2 tail current, assuming $R_s = 10$ $\Omega \cdot$ cm^2 [20].

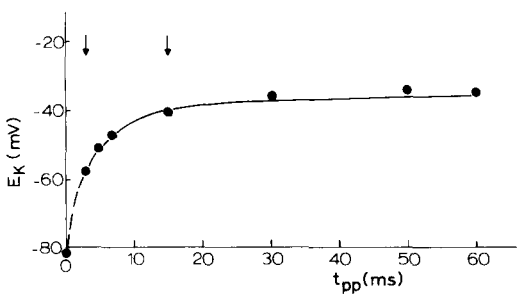

Fig. 2. Potassium reversal potential, E_K, as a function of a depolarizing prepulse duration, t_{pp} ($E_{pp} = +86$ mV). Circles correspond to the experimental values of E_K. Continuous line, calculated from the outward I_K using the three-compartment model with the following parameters: $P_{Ks} = 3.0 \cdot 10^{-4}$ cm/s, $\theta = 123$ Å, evaluated from the experimental data in the region delimited by the arrows. The reconstruction started at the first experimentally determined E_K (here, $t_{pp} = 3$ ms).

Anatomical structure of Myxicola axon

Our conclusion as to the similarity in the potassium accumulation between *Myxicola* and the squid resulting from similar compartmentalization gains support from morphological studies. Fig. 3 shows electron micrographs of the giant axon of *Myxicola* and the adjacent Schwann cell layer. The width of the anatomical periaxonal space (Fig. 3B) is 10–20 nm, comparable to that determined electrophysiologically. The thickness of the Schwann cell layer is about 10 μm (Fig. 3A), approx. 10-times that in the squid [15]. In addition, the mesaxonal clefts seem to be even more tortuous than those in the squid periaxonal sheath, yielding about 20-times longer effective pathlength in *Myxicola*. However, there are roughly 10-times more mesaxons per unit periaxonal surface in *Myxicola* axon than in squid axon (compare Fig. 3 here with Figs. 1 and 4 in Ref. 15). The width of the mesaxonal clefts is approx. 25 nm (Fig. 3C), i.e., about 2.5-times larger than in the squid [15]. Therefore, the mesaxonal area abutting the periaxonal space and the basal lamina in *Myxicola* is roughly 25-times larger than in squid.

Calculation of Schwann cell layer resistance from morphological data

These anatomical features can be used to calculate the electrical resistance, R, across the periaxonal sheath, with the branching mesaxonal clefts approximated to a truncated cone-shaped volume conductor [15] normalized to 1 cm^2 of axon surface, A:

$$R = \frac{\rho h A}{\pi r_1 r_2} \tag{3}$$

where ρ is the specific resistivity of the conducting medium, assumed here to equal that of sea-water, 25 $\Omega \cdot$ cm; h is the length of the shortest mesaxonal cleft, and r_1 and r_2 are the radii of the cone at the periaxonal space and at the basal lamina, respectively.

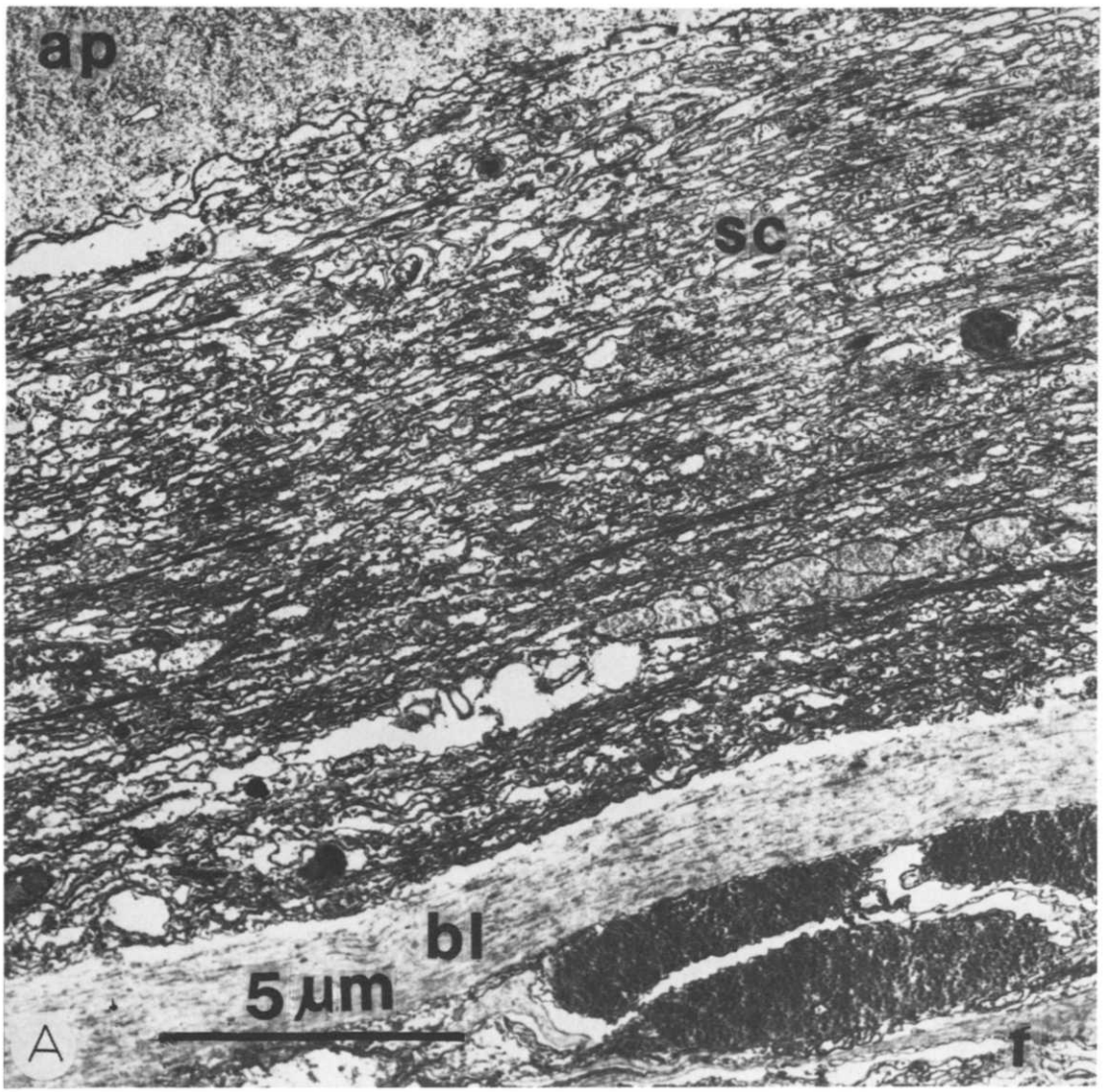

Fig. 3. (See also facing page.) Electron micrograph of a cross-section of a giant axon of *Myxicola* and the adjacent periaxonal layer. (A) Schwann cells (sc; note the thickness of this layer); ap, axoplasm; bl, basal lamina; f, fibroblasts. (B) Mesaxonal clefts (ma) branching from the periaxonal space (ps) adjacent to the axolemma (al). (C) Note the tortuousity of mesaxonal clefts.

Introducing the aforementioned differences between *Myxicola* and squid, i.e., h about 20-times larger and both r_1 and r_2 about 5-times larger, gives the value of about 0.7 $\Omega \cdot cm^2$, which is similar to the value of 0.9 $\Omega \cdot cm^2$ for squid [15].

Consistency with values of barrier resistance determined by other means

This value of R relates to that of 2.9 ± 0.5 $\Omega \cdot cm^2$ calculated from our electrophysiological data by the following relationship [2]:

$$R_s = \rho D / P_{Ks} \tag{4}$$

with ρ as previously defined, D, the diffusion coefficient in sea-water, of $1.5 \cdot 10^{-5}$ cm^2/s and a steady-state P_{Ks} value of $(1.3 \pm 0.4) \cdot 10^{-4}$ cm/s. A value of R_s of 4.6 ± 1.2 $\Omega \cdot cm^2$ has been determined directly from current-clamp measurements in *Myxicola* [20]. This value and the value of

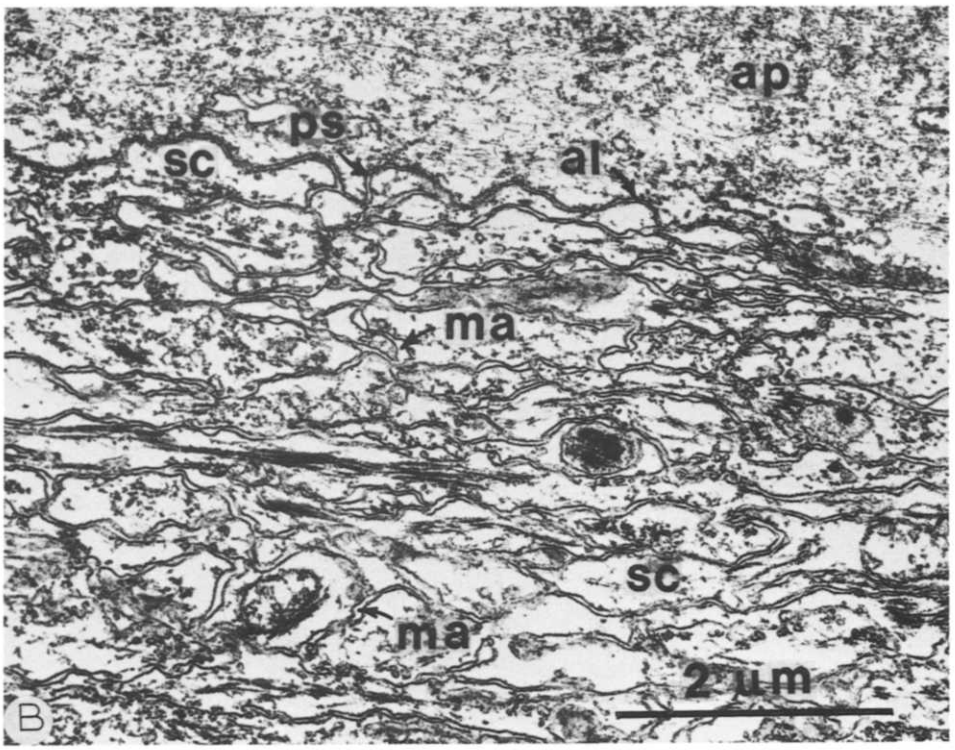
ap
ps
sc
al
ma
sc
ma
2 µm
B

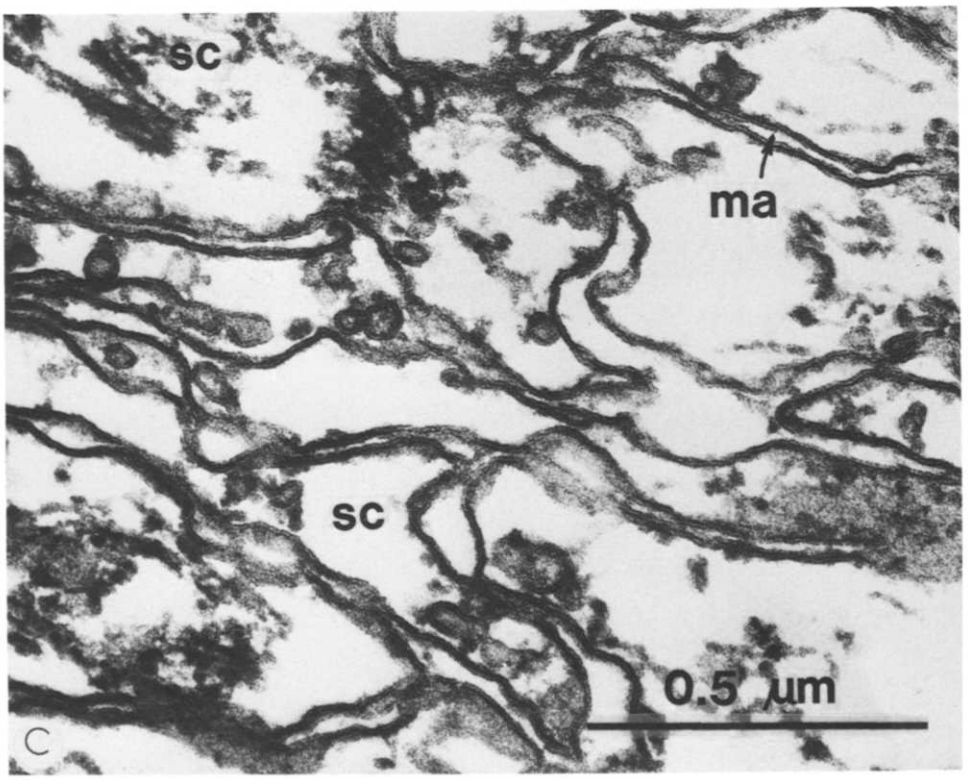
sc
ma
sc
0.5 µm
C

R_s calculated from P_{Ks} should be larger than the value of R_s based on the anatomical structure of the Schwann cell layer, because these former values include additional contributions from the basal lamina, connective tissue and fibroblast layer and the outer perineural layer. The current-clamp R_s measurement also includes, in addition to the above, the contribution to R_s from the axoplasmic resistance which is higher in *Myxicola* than in the squid [22,20].

References

1 Barry, P.H. and Hope, A.B. (1969) Biophys. J. 9, 700–728
2 Frankenhaeuser, B. and Hodgkin, A.L. (1956) J. Physiol. 131, 341–376
3 Palti, Y., Adelman, W.J., Jr. and Senft, J.P. (1972) Actual. Neurophysiol. 10, 210–235
4 Adelman, W.J., Jr., Palti, Y. and Senft, J.P. (1973) J. Membrane Biol. 13, 387–410
5 Palti, Y., Stampfli, R., Bretag, A. and Nonner, W. (1973) Isr. J. Med. Sci. 9, 680a
6 Moran, N., Palti, Y., Levitan, E. and Stampfli, R. (1980) Biophys. J. 32, 939–954
7 Binstock, L. and Goldman, L. (1971) J. Physiol. 217, 517–531
8 Begenisich, T. (1975) J. Gen. Physiol. 66, 47–65
9 Carbone, E., Fioravanti, L., Prestipino, G. and Wanke, E. (1978) J. Membrane Biol. 43, 295–315
10 Moran, N., Palti, Y., Levitan, E. and Binah, O. (1979) Isr. J. Med. Sci. 15, 619a
11 Binstock, L. and Goldman, L. (1969) J. Gen Physiol. 54, 730–740
12 Adelman, W.J., Jr. and Palti, Y. (1969) J. Gen. Physiol. 53, 685–691
13 Goldman, L. and Binstock, L. (1969) J. Gen. Physiol. 54, 755–764
14 Hodgkin, A.L. and Huxley, A.F. (1952) J. Physiol. 117, 500–544
15 Adelman, W.J., Jr., Moses, J. and Rice, R.V. (1977) J. Neurocytol. 6, 621–646
16 Villegas, G.M. (1969) J. Ultrastruct. Res. 26, 501–514
17 Adelman, W.J., Jr. and Palti, Y. (1972) in Current Topics in Membranes and Transport (Bronner, F. and Kleinzeller, A., eds.), Vol. III, pp. 199–235, Academic Press, New York
18 Adams, G. (1973) J. Membrane Biol. 13, 353–386
19 Taylor, R.E., Bezanilla, F. and Rojas, E. (1980) Biophys. J. 29, 95–218
20 Binstock, L., Adelman, W.J., Jr., Senft, J.P. and Lecar, H. (1975) J. Membrane Biol. 21, 25–47
21 Gilbert, D.S. and Shaw, T.I. (1969) J. Physiol. 204, 28–29P
22 Carpenter, D.O., Hovey, M.M. and Bak, A.F. (1972) Society for Neurosciences, Second Annual Meeting (Abstr.)